1521-0111/96/4/475–484$35.00
MOLECULAR PHARMACOLOGY

https://doi.org/10.1124/mol.119.117259
Mol Pharmacol 96:475–484, October 2019

Intercalating TOP2 Poisons Attenuate Topoisomerase Action at Higher Concentrations[S]

Mandeep Atwal, Rebecca L. Swan, Chloe Rowe, Ka C. Lee, David C. Lee, Lyle Armstrong, Ian G. Cowell, and Caroline A. Austin

Institute for Cell and Molecular Biosciences, Newcastle University, Newcastle upon Tyne, United Kingdom (M.A., R.L.S., C.R., K.C.L., I.G.C., C.A.A.) and Institute of Genetic Medicine, Newcastle University, International Centre for Life, Central Parkway, Newcastle upon Tyne, United Kingdom (D.C.L., L.A.)

Received May 16, 2019; accepted August 2, 2019

ABSTRACT

Topoisomerase II (TOP2) poisons are effective cytotoxic anticancer agents that stabilize the normally transient TOP2-DNA covalent complexes formed during the enzyme reaction cycle. These drugs include etoposide, mitoxantrone, and the anthracyclines doxorubicin and epirubicin. Anthracyclines also exert cell-killing activity via TOP2-independent mechanisms, including DNA adduct formation, redox activity, and lipid peroxidation. Here, we show that anthracyclines and another intercalating TOP2 poison, mitoxantrone, stabilize TOP2-DNA covalent complexes less efficiently than etoposide, and at higher concentrations they suppress the formation of TOP2-DNA covalent complexes, thus behaving as TOP2 poisons at low concentration and inhibitors at high concentration. We used induced pluripotent stem cell (iPSC)–derived human cardiomyocytes as a model to study anthracycline-induced damage in cardiac cells. Using immunofluorescence, our study is the first to demonstrate the presence of topoisomerase IIβ (TOP2B) as the only TOP2 isoform in iPSC-derived cardiomyocytes. In these cells, etoposide robustly induced TOP2B covalent complexes, but we could not detect doxorubicin-induced TOP2-DNA complexes, and doxorubicin suppressed etoposide-induced TOP2-DNA complexes. In vitro, etoposide-stabilized DNA cleavage was attenuated by doxorubicin, epirubicin, or mitoxantrone. Clinical use of anthracyclines is associated with cardiotoxicity. The observations in this study have potentially important clinical consequences regarding the effectiveness of anticancer treatment regimens when TOP2-targeting drugs are used in combination. These observations suggest that inhibition of TOP2B activity, rather than DNA damage resulting from TOP2 poisoning, may play a role in doxorubicin cardiotoxicity.

SIGNIFICANCE STATEMENT

We show that anthracyclines and mitoxantrone act as topoisomerase II (TOP2) poisons at low concentration but attenuate TOP2 activity at higher concentration, both in cells and in in vitro cleavage experiments. Inhibition of type II topoisomerases suppresses the action of other drugs that poison TOP2. Thus, combinations containing anthracyclines or mitoxantrone and etoposide may reduce the activity of etoposide as a TOP2 poison and thus reduce the efficacy of drug combinations.

Introduction

Human type II DNA topoisomerases (TOP2) are highly effective anticancer drug targets, but TOP2-targeting drugs (TOP2 poisons) can cause short- and long-term side effects, including neutropenia, therapy-related leukemia, and cardiotoxicity (Cowell and Austin, 2012; De Angelis et al., 2016). Anthracyclines target TOP2 and act via additional mechanisms, including lipid peroxidation, redox activity, and drug-DNA cross-link formation (Winterbourn et al., 1985; Bodley et al., 1989; Sinha et al., 1989; Capranico et al., 1990a; Gewirtz, 1999; Swift et al., 2006; Coldwell et al., 2008). However, they can induce serious complications in cardiac and myeloid cells even at doses under the maximum recommended lifetime exposure limit. Tailored tests are reducing the number of patients receiving cytotoxic chemotherapy (Sparano et al., 2018), but anthracycline-containing chemotherapy regimens are still recommended for many patients, including children and adolescents. Thus, it is important to understand the mechanism by which the adverse effects arise to be able to modify current treatment regimens to reduce side effects. Recently, topoisomerase IIβ (TOP2B) was implicated in cardiotoxicity, as murine cardiomyocytes lacking TOP2B are protected from doxorubicin damage (Zhang et al., 2012).

Drugs that target TOP2 fall into at least two categories: TOP2 poisons such as etoposide (Long et al., 1984) and catalytic inhibitors such as ICRF-187 (dexrazoxane) ((S)-4,4'-(propane-1,2-diyl)bis(piperazine-2,6,-dione) (Roca et al., 1994; Classen et al., 2003). TOP2 poisons stabilize the TOP2-DNA covalent complex when DNA is in the cleaved position, leading

This work was supported by Breast Cancer Now [Grant 2012NovemberPhD11] and Bloodwise [Programme Grant 12031, Gordon Piller Studentship 13063].
https://doi.org/10.1124/mol.119.117259.
[S] This article has supplemental material available at molpharm.aspetjournals.org.

ABBREVIATIONS: DAPI, 4′,6-diamidino-2-phenylindole; dox, doxorubicin; DSB, double-strand break; epi, epirubicin; ICRF-193, 4-[2-(3,5-dioxo-1-piperazinyl)-1-methylpropyl]piperazine-2,6-dione; iPSC, induced pluripotent stem cell; kDNA, kinetoplast DNA; Pen/Strep, penicillin/streptomycin; TARDIS, trapped in agarose DNA immunostaining assay; TOP2, topoisomerase II; TOP2A, topoisomerase IIα; TOP2B, topoisomerase IIβ.

to the accumulation of TOP2-DNA complexes within the cell that can result in cell death (Cowell and Austin, 2012). TOP2 catalytic inhibitors antagonize the action of TOP2 poisons and, therefore, may be used in combination with TOP2 poisons to reduce the side effects arising from TOP2 poison therapy (Reichardt et al., 2018).

Early in vitro studies and in cellulo studies of anthracycline interactions with TOP2 found a bell-shaped concentration dependence in the induction of DNA cleavage (Capranico et al., 1990a,b; Ferrazzi et al., 1991; Willmore et al., 2002). In vitro cleavage on pBR322 DNA showed doxorubicin cleavage at low concentrations, but less at higher concentrations (Tewey et al., 1984). The same effect was observed using in vitro end-labeled PMC41 DNA in cleavage assays (Bodley et al., 1989) or in vitro end-labeled SV40 DNA (Binaschi et al., 1998). In addition to suppression of in vitro cleavage, higher concentrations of doxorubicin and epirubicin attenuated teniposide and amsacrine (Capranico et al., 1990a,b). These early in vitro cleavage experiments used topoisomerase II enzyme purified from murine L1210 cells, which contained a mixture of the two isoforms topoisomerase IIα (TOP2A) and TOP2B. Using SDS/KCl to precipitate protein-DNA complexes, doxorubicin stabilized fewer protein-DNA complexes compared with an equitoxic dose of etoposide in the rat glioblastoma cell line C6 (Montaudon et al., 1997); no accumulation of TOP2-DNA complexes was observed in KB cells following doxorubicin treatment (Suzuki et al., 1997). Using immunologic assays specific for TOP2-DNA complexes, such as the trapped in agarose DNA immunostaining assay (TARDIS) and the in vivo complex of enzyme assay, which produce robust signals when cells are treated with etoposide, TOP2-DNA complexes were detectable under some conditions with mitoxantrone, idarubicin, epirubicin, and doxorubicin (Willmore et al., 2002; Errington et al., 2004; Smart et al., 2008; Hasinoff et al., 2016; Atwal et al., 2017). In this study, using the TARDIS assay, we confirm that mitoxantrone, doxorubicin, and epirubicin stabilize covalent TOP2-DNA complexes at lower concentrations, demonstrating poisoning activity, but that fewer complexes are stabilized at higher concentrations in cells, indicating inhibition of activity. Inhibition by mitoxantrone, doxorubicin, and epirubicin was compared with the catalytic inhibitor ICRF-193 (4-[2-(3,5-dioxo-1-piperazinyl)-1-methylpropyl]piperazine-2,6-dione). In vitro experiments using recombinant TOP2A or TOP2B demonstrated that decatenation by either isoform was inhibited by mitoxantrone, doxorubicin, or epirubicin and that etoposide-induced cleavage by either isoform was attenuated by mitoxantrone, doxorubicin, or epirubicin. Biphasic poisoning/inhibition of TOP2 has potential implications for the pharmacokinetics of anthracyclines in cancer therapy.

Materials and Methods

Reagents and Antibodies. Doxorubicin, epirubicin, etoposide and mitoxantrone, dimethylsulfoxide, Tween 20, Triton X-100, and paraformaldehyde were purchased from Sigma-Aldrich (Dorset, UK). ICRF-193 was purchased from Biomol (Hamburg, Germany). Kinetoplast DNA (kDNA) was purchased from Inspiralis (Norwich, UK). Plasmid TCS1 was a gift from T. Hsieh, Duke University (Durham, NC) (Lee et al., 1989), and supercoiled plasmid DNA was purified using caesium chloride centrifugation. Recombinant human TOP2A and human TOP2B were produced as described by Wasserman et al. (1993) and West et al. (2000). Anti-TOP2 polyclonal antibodies raised in rabbits were used to conduct experiments. 4882 Anti-TOP2 was raised to topoisomerase II purified from calf thymus; this protein was a ~140-kDa N-terminal fragment lacking the C-terminal region based on partial peptide sequencing, and was a mixture of TOP2A and TOP2B (Austin et al., 1990). Antibodies 4566 and 4555 were raised to the C-terminal domain of recombinant human TOP2A (residues 1244–1531) or recombinant human TOP2B (residues 1263–1621), respectively. These antibodies were developed in house (see Supplemental Fig. 1). Anti-mouse γH2AX (catalog number 05-636) was obtained from Merck-Millipore.

Decatenation Assays. Two Hundred nanograms of kDNA was incubated in reaction buffer [50 mM Tris-HCl (pH 7.5), 125 mM NaCl, 10 mM $MgCl_2$, 5 mM Dithiothreitol, and 100 μg/ml albumin], with or without drug, as indicated in the figure legends; the reaction volume was 20 μl, and reactions were initiated by the addition of TOP2A or TOP2B and incubated for 30 minutes at 37°C. Loading buffer was added and samples were run on a 0.8% gel in TBE buffer [100 mM Tris-borate (pH 8.3), 2 mM EDTA]. Gels were stained with ethidium bromide after electrophoresis and visualized on a Bio-Rad EZ gel doc.

DNA Cleavage Assays. pTCS1 DNA substrate (3.9 μg) was incubated in reaction buffer [10 mM Tris-HCl (pH 8.0), 10 mM $MgCl_2$, 50 mM KCl, 150 μg/ml bovine serum albumin, and 1 mM ATP] in the presence or absence of mitoxantrone, doxorubicin, or epirubicin with or without etoposide for 30 minutes at 37°C. The reactions were initiated by the addition of 1.2 μg of TOP2A or TOP2B, and the reaction volume was 100 μl. Reactions were terminated by addition of SDS to 1%, followed by addition of EDTA to 25 mM and proteinase K to 0.5 mg/ml, and incubated for 60 minutes at 45°C. The DNA was precipitated overnight at −20°C following the addition of sodium acetate to 300 mM and the addition of two volumes of ethanol. The DNA precipitate was collected by centrifugation and the pellet air dried prior to resuspension in 15 μl TE buffer [10mM Tris-HCl, 1mM EDTA (pH 8.0)]; 5 μl of loading buffer was added, and the samples were heated to 70°C for 2 minutes prior to running on a 0.8% agarose gel in TAE buffer [40 mM Tris, 2 mM EDTA and 0.11% (v/v) glacial acetic acid (pH 8.3)] in the presence of ethidium bromide. Gels were visualized on a Bio-Rad EZ gel doc and bands were quantified by ImageLab v.5.2.1 (Bio-Rad).

Cell Culture. NB4 and K562 cells were maintained in RPMI 1640 medium supplemented with 10% fetal bovine serum and 1% penicillin and streptomycin (Thermo Fisher Scientific, Paisley, UK). Cells were cultured at 37°C in a humidified atmosphere containing 5% CO_2. Experiments were conducted on exponentially growing cells (2–5 × 10^5 cells/ml). NB4 (ACC-207) and K562 (CCL-243) cell lines (Lozzio and Lozzio, 1975; Lanotte et al., 1991) were originally sourced from the German Collection of Microorganisms and Cell Cultures GmbH and American Type Culture Collection, respectively. Cells were routinely tested for mycoplasma infection.

Undifferentiated induced pluripotent stem cells (iPSCs) were maintained in feeder-free culture with GFR Matrigel (Corning) and mTeSR1 (StemCell Technologies, Cambridge, UK) with 1% penicillin/streptomycin (Pen/Strep); these cells were tested monthly for mycoplasma and were originally sourced from Lonza (Basel, Switzerland). Differentiation to induced pluripotent stem cell–derived cardiomyocytes was performed using an established protocol followed by metabolic purification (Lian et al., 2013; Tohyama et al., 2013). In brief, iPSCs were cultured as described earlier to form a confluent monolayer; at this point (day 1 of the protocol), the medium was changed to a base differentiation medium consisting of RPMI 1640 supplemented with B27 minus insulin and 1% Pen/Strep (Life Technologies) and 9 μM CHIR99021 trihydrochloride (Tocris, Abingdon UK). On day 2, the medium was changed to base medium. On day 4, the medium was changed to a mixture of fresh basal medium and the existing medium from the culture in a 1:1 ratio; this was supplemented with 5 μM IWP2 (Tocris). The medium was changed to base medium on day 6, and on day 8 the medium was changed to

maintenance medium consisting of RPMI 1640 supplemented with 2% B27 and 1% Pen/Strep. On day 10, the medium was changed to metabolic purification medium consisting of RPMI 1640 without glucose, supplemented with 2% B27 and 1% Pen/Strep. On day 15, the medium was replaced with maintenance medium. Thereafter, the maintenance medium was changed every 2 to 3 days. Cardiomyocytes generated using this protocol were characterized by fluorescence-activated cell sorter analysis of SIRPA gene expression (Dubois et al., 2011) followed by quantitative polymerase chain reaction quantification of sarcomeric marker genes (ACTN2, TNNT2, TNNI3, MYH6, and MYH7) and detection of their respective proteins by immunohistochemistry (data not shown). Cardiomyocyte function was assessed by observation of spontaneous contraction and recording spontaneous calcium transients.

TARDIS Assay. The TARDIS assay was used to quantify the level of stabilized TOP2-DNA covalent complexes in situ, conducted as previously described (Willmore et al., 1998; Cowell et al., 2011). In brief, cells were treated for 1 hour with the desired TOP2 poison. Cells were pelleted (1000*g*, 5 minutes) and washed in ice-cold PBS. After recentrifugation, cells were mixed in an equal volume of molten 2% low melting point agarose (Lonza) in PBS and spread evenly onto agarose-coated slides. Agarose-embedded cells were lysed [1% (w/v) SDS, 20 mM sodium phosphate, 10 mM EDTA, pH 6.5], and noncovalently bound DNA proteins were removed using 1 M NaCl. Stabilized TOP2 covalent complexes were detected by immunofluorescence using anti-TOP2 rabbit polyclonal antibodies followed by Alexa Fluor 488–coupled anti-rabbit secondary antibodies (Thermo Fisher Scientific). Slides were counterstained with Hoechst 33258 (Thermo Fischer Scientific) to visualize DNA. Images were captured for Hoechst 33258 and Alexa Fluor 488 using an epifluorescence microscope (IX-81, 10× objective; Olympus) fitted with an Orca-AG camera (Hamamatsu) and suitable narrow-band filter sets. Image capture and automated slide scoring was performed using Volocity 6.3 software (PerkinElmer). In brief, acquired images were each processed to identify nuclei by thresholding the Hoechst 33258 signal. After filtering to separate or remove touching/overlapping objects (nuclei), the immunofluorescent signal emanating from each nucleus was determined to produce a table of integrated fluorescence per nucleus. Parameters to select individual nuclei were set up at the beginning of the analysis for one slide, and these parameters were then used for all other slides in the experiment. Data are represented using GraphPad Prism 8.0 or 8.1 (GraphPad Software) and R (The R Foundation, San Diego, CA).

Immunofluorescence Analysis of γH2AX. After drug treatment, cells were washed and pelleted in ice-cold PBS and spotted on poly-L-lysine–coated slides. Cells were fixed in 4% paraformaldehyde in PBS for 10 minutes and permeabilized using KCM+T buffer [120 mM KCl, 20 mM NaCl, 10 mM Tris-HCl (pH 8.0), 1 mM EDTA, 0.1% Triton X-100] for 15 minutes. After blocking in (KCM+T, 2% bovine serum albumin, 10% dry milk powder), cells were probed with anti-γH2AX in blocking buffer followed by Alexa Fluor 594 anti-mouse secondary antibodies. Slides were counterstained with DAPI (4',6 diamidine 2 phenylindole). Images were captured for DAPI and Alexa Fluor 594 and quantification was performed using Volocity 6.3 (PerkinElmer) as described for the TARDIS assay.

Statistics. Statistical analysis was performed using GraphPad Prism 8.0. The details of the tests performed are given in the figure legends. For signifying P values, * refers to $P < 0.05$, ** refers to $P < 0.01$, *** refers to $P < 0.001$, and **** refers to $P < 0.0001$. NS indicates not significant. Error bars in bar charts represent S.D. values. The study was designed to be exploratory rather than testing a specific null hypothesis, and therefore, P values are descriptive only. Where intergroup comparisons were made, these were specified in advance of data acquisition. Sample sizes (numbers of replicate experiments) were specified in advance of data acquisition based on prior knowledge of the characteristics of the assays involved and anticipating occasional lost or failed samples.

Results

Etoposide and Mitoxantrone Both Induce Stable TOP2-DNA Complexes but with Differing Concentration Responses. TOP2-DNA covalent complexes stabilized by TOP2 poisons, such as etoposide, can be efficiently and specifically detected using the TARDIS assay (Willmore et al., 1998; Cowell et al., 2011). In this assay, cells treated with TOP2 poison are suspended in low-melting-point agarose, spread on glass microscope slides, and lysed in buffer containing 1% SDS and then extracted in high-salt buffer. This treatment removes most cellular constituents, leaving "nuclear ghosts" trapped in the agarose which consist of nuclear DNA and any covalently attached proteins. TOP2A or TOP2B covalent DNA complexes can then be detected and quantified on a single cell basis by immunofluorescence. In this way, the median fluorescent signal per nucleus and the distribution of nuclear signal intensities can be determined. For the archetypal epipodophyllotoxin TOP2 poison etoposide, TOP2A complexes can be reproducibly detected with as little as 1 μM etoposide, and TOP2B complex induction can be detected from 10 μM in mouse and human cells (Willmore et al., 1998; Cowell et al., 2011; Atwal et al., 2017) (Fig. 1A). TOP2 complex levels increased with increasing etoposide concentration up to at least 100 μM etoposide. TOP2 complexes are processed in the cell to give rise to DNA double-strand breaks (DSBs) that elicit a DNA damage response, including the phosphorylation of histone H2AX. Etoposide-induced levels of H2AX phosphorylation followed a dose response similar to that observed for TOP2-DNA complexes (Fig. 1B).

Mitoxantrone is an anthracenedione TOP2 poison that, unlike etoposide, intercalates into DNA with a high affinity (Lown et al., 1984). We have previously shown that mitoxantrone also efficiently induces both TOP2A- and TOP2B-DNA complexes in murine cells, but the quantity of complexes plateaus at approximately 1 μM mitoxantrone (Errington et al., 1999). We confirm this result here using human NB4 cells (Fig. 1C) and demonstrate that, at a higher concentration (20 μM), TOP2A and TOP2B complex levels are reduced, suggesting that mitoxantrone inhibits TOP2-DNA complex formation at elevated concentrations. This reduction in TOP2-DNA complexes at higher concentrations of mitoxantrone was mirrored in the level of H2AX phosphorylation. Levels of γH2AX signal peaked with 1 μM mitoxantrone and decreased at 10 and 20 μM mitoxantrone (Fig. 1D).

Anthracyclines Targeting TOP2 Are Inefficient at Inducing Stable TOP2-DNA Complexes. Similar to etoposide and mitoxantrone, anthracyclines, including doxorubicin (dox) and epirubicin (epi), are TOP2 poisons on the basis of their ability to increase the steady-state concentration of the covalent TOP2-DNA complexes by impeding religation of DNA (Pommier et al., 2010; Vos et al., 2011). Each of these drugs stimulates cleavage of DNA substrates by TOP2 in in vitro assays (Bodley et al., 1989; Capranico et al., 1993; Binaschi et al., 1998). However, unlike etoposide and mitoxantrone, the anthracyclines have not been reported to induce the formation of large numbers of stable TOP2-DNA complexes in cells that can be detected using the TARDIS assay or the in vivo complex of enzyme assay (Montaudon et al., 1997; Willmore et al., 2002; Swift et al., 2006; Nitiss et al., 2012). For example, while the anthracycline idarubicin induced a small

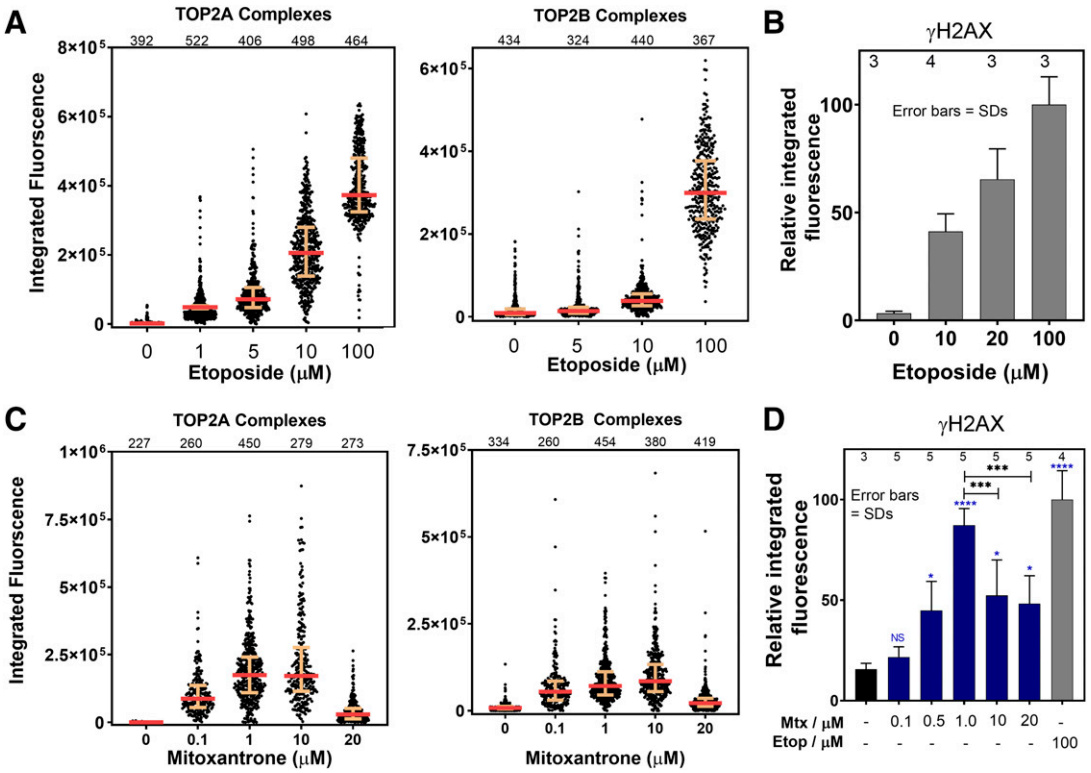

Fig. 1. Dose response for formation of TOP2-DNA complexes and histone H2AX phosphorylation induced by etoposide (Etop) and mitoxantrone (Mtx). (A) NB4 cells were treated with the indicated concentrations of etoposide. TOP2A and TOP2B complexes were quantified on a cell-by-cell basis by the TARDIS assay using anti-TOP2A (4566) or anti-TOP2B (4555), respectively. Data are displayed as scatterplots, each dot representing the integrated immunofluorescent signal from a single nucleus. Medians and interquartile ranges are indicated. The number of nuclei quantified for each condition are indicated above each plot. For TOP2A, fluorescent intensities were significantly above those of untreated cells for 1 μM etoposide and above, whereas for TOP2B, significant increase was reached by 10 μM. (B) Cells treated as in (A) were analyzed by immunofluorescence for phospho-S_{139} histone H2AX (γH2AX). The results are displayed as the means of the medians of replicate experiments (number of replicas indicated above each bar) normalized to 100 μM etoposide. Error bars represent the S.D. (C and D) NB4 cells were treated with the indicated concentrations of mitoxantrone and were analyzed for TOP2-DNA complexes and γH2AX immunofluorescence as in (A) and (B), respectively. For both TOP2A and TOP2B, fluorescent intensities significantly increased compared with untreated cells at all concentrations of mitoxantrone from 0.1 to 20 μM. (D) Significance values were determined using one-way ANOVA with Tukey correction for multiple comparisons. Significance values shown in blue refer to comparison with untreated cells. Error bars indicate S.D. values.

dose-dependent increase in TOP2A complexes up to 1 μM and a marginal increase in TOP2B complexes over control cells, at 20 μM fewer TOP2-DNA complexes were seen (Willmore et al., 2002). Doxorubicin-induced TOP2-DNA complexes were not detected in this previous TARDIS study (Willmore et al., 2002).

In this study, we were able to detect doxorubicin- and epirubicin-induced TOP2A complexes in human NB4 cells using the TARDIS assay (Fig. 2A). This discrepancy may be due to the improved sensitivity of the assay in the current study resulting from the use of brighter, more stable fluorochromes and more sensitive camera technology. However, median fluorescence levels per nucleus did not exceed 20% of the level recorded for the positive control treatment (100 μM etoposide), and no significant dox or epi signal was observed for TOP2B (Fig. 2A). For both dox and epi, only a small increase in median fluorescent signal was observed for TOP2A between 1.0 and 10 μM. Subsequent experiments were carried out at 10 μM for both drugs. In line with the reduced level of stabilized TOP2 complexes compared with 100 μM etoposide, dox and epi both resulted in lower γH2AX induction than etoposide (Fig. 2B). This is similar to a previous finding (Huelsenbeck et al., 2012) in rat glioblastoma cells, where doxorubicin-induced H2AX phosphorylation was maximal at 2 μM and was reduced compared with the extent of phosphorylation induced by 100 μM etoposide. Since TARDIS analysis provides fluorescence intensity data from individual nuclei, the resulting data can also be presented as the percentage of cells with a signal above a given threshold (Huelsenbeck et al., 2012). We chose 25% of the value of the median signal obtained for 100 μM etoposide as a convenient threshold. For TOP2A (4566), approximately 5% and 10% of 10 μM dox- and epi-treated cells exceeded this cutoff (Fig. 2C).

The data obtained for Figs. 1 and 2 involved treating cells for 60 minutes with TOP2 poison before carrying out the TARDIS assay. To determine whether the relatively low level of stable TOP2-DNA complexes observed with epi was due to slow complex formation compared with etoposide, a TOP2A TARDIS time-course experiment was performed. Median fluorescence levels induced by epi did not increase with drug incubation times from 30 to 120 minutes (Fig. 3A). The TARDIS assay data shown in Figs. 1, 2, and 3A used antibodies raised to the divergent C-terminal regions of the TOP2A and TOP2B proteins, which allows the two isoforms to be analyzed independently (4566 and 4555, respectively; see Supplemental Fig. 1). We were concerned that the low signal observed with the anthracyclines compared with etoposide could be due to epitope masking by post-translational

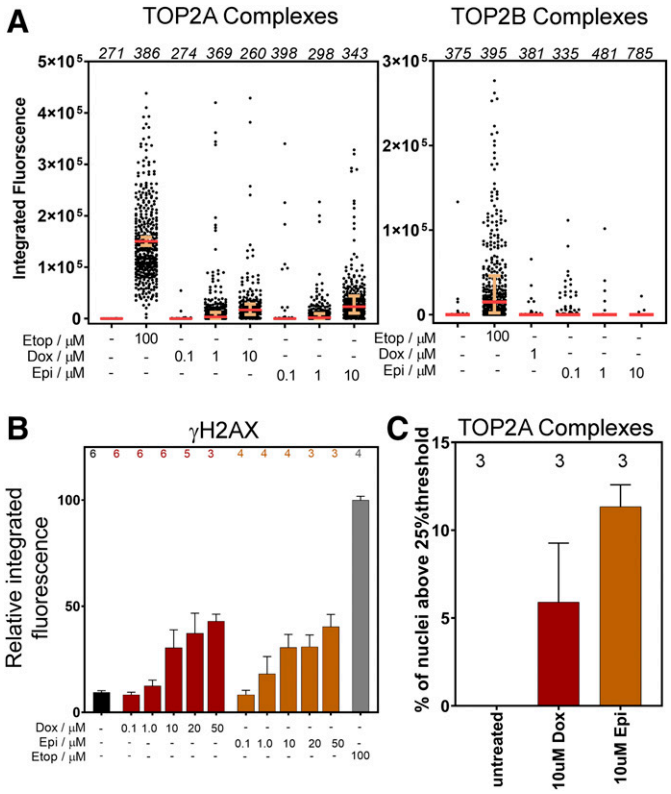

Fig. 2. Dose response for formation of TOP2-DNA complexes and histone H2AX phosphorylation induced by doxorubicin and epirubicin. (A) NB4 cells were treated with the indicated concentrations of anthracycline or etoposide (Etop). TOP2A- and TOP2B-DNA complexes were quantified as in Fig. 1. The number of cells analyzed for each treatment is indicated in italics at the top of each graph. (B) Cells were treated as in (A) and were analyzed by immunofluorescence for γH2AX. The results are displayed as the means of the medians of replicate experiments ±S.D, normalized to 100 μM etoposide. The number of replicates for each condition is indicated above each graph. (C) Proportion of cells treated with 10 μM dox or epi that exhibit TOP2A TARDIS fluorescence above a threshold of 25% of the median value obtained with 100 μM etoposide. Error bars indicate S.D. values.

modification or rapid proteolytic removal of the C-terminal domain following anthracycline drug treatment. To test this possibility, we repeated the TARDIS assay with antibody 4882, which was raised to the conserved N-terminal 140 kDa of calf thymus TOP2 and detects both isoforms of human TOP2 (see Supplemental Fig. 1). Using this antibody, 10 and 100 μM etoposide produced a robust signal in the TARDIS assay. However, no significant increase in median fluorescence was observed for 10 μM dox or epi compared with the no-drug control (Fig. 3, B and C), whereas an intermediate level of signal was observed for 20 μM mitoxantrone. Considering the results obtained with antibodies 4566 (TOP2A C-terminal domain), 4555 (TOP2B C-terminal domain), and 4882 (TOP2A and TOP2B N-terminal 140 kDa), the low anthracycline-induced TOP2A signal and lack of TOP2B signal in the TARDIS assay are not likely to be due to loss or masking of the C-terminal domain, indicating inefficient trapping of stable TOP2 complexes by dox and epi.

Doxorubicin, Epirubicin, and Mitoxantrone Can Inhibit Stable TOP2-DNA Complexes in Competition Assays. Various lines of evidence, including in vitro DNA cleavage data, H2AX phosphorylation, and TARDIS data (Bodley et al., 1989; Willmore et al., 2002; Smart et al., 2008; Huelsenbeck et al., 2012), support the idea that intercalating anthracycline TOP2 poisons and mitoxantrone inhibit TOP2 activity at higher concentrations. Competition between poisoning and inhibition may then explain the relatively inefficient generation of stable TOP2-DNA complexes by anthracyclines. To further study this, etoposide-induced TOP2 complexes were quantified using the TARDIS assay in NB4 cells that had been preincubated with 10 μM dox, 10 μM epi, 20 μM mitoxantrone, or the well characterized bisdioxopiperazine TOP2 catalytic inhibitor ICRF-193 (100 μM) (Patel et al., 2000). As noted previously, the anthracyclines on their own induced a low TOP2A signal compared with that obtained with etoposide, whereas 20 μM mitoxantrone alone induced a small but significant TOP2A signal. ICRF-193 did not induce TOP2A or TOP2B complexes significantly above basal levels. However, preincubation with each of these drugs significantly inhibited both TOP2A and TOP2B covalent complex formation by etoposide (Fig. 4, A and B). Indeed, the level of inhibition achieved by the anthracyclines and mitoxantrone was similar to that observed for ICRF-193. Since NB4 cells contain a high level of myeloperoxidase activity, which increases TOP2 complex formation via oxidative activation of etoposide, we repeated the experiments shown in Fig. 4, A and B using the myeloperoxidase nonexpressing cell line K562 (Fig. 4, C and D). Very similar results were observed in K562 cells; the anthracyclines efficiently inhibited etoposide-induced TOP2A and TOP2B complex formation at 10 and 100 μM etoposide. Mitoxantrone also significantly inhibited etoposide-induced TOP2B complex formation and TOP2A complexes at 100 μM etoposide.

Since TOP2 complexes are processed in cells to DSBs that elicit γH2AX formation, we also determined the ability of dox, epi, and mitoxantrone to inhibit etoposide-induced H2AX phosphorylation. As observed in Fig. 2B, the anthracyclines alone at 10 μM led to H2AX phosphorylation (Fig. 5); however, no signal above background was observed for 100 μM ICRF-193. Levels of histone H2AX phosphorylation induced by 10 μM etoposide were not significantly increased or decreased by pretreatment with dox or epi compared with etoposide alone. Whereas dox and epi alone produce an H2AX signal, no additive effect on DSB formation was observed when the anthracyclines were coincubated with 10 μM etoposide. In addition, H2AX phosphorylation induced by 10 μM etoposide was not reduced by anthracycline treatment. However, preincubation with epi, but not dox, did significantly reduce the level of H2AX phosphorylation by approximately 25% following treatment with 100 μM etoposide. In contrast, etoposide-induced H2AX phosphorylation was strongly suppressed by mitoxantrone at both concentrations of etoposide. Indeed, this suppression was greater than that observed for ICRF-193 with 100 μM etoposide, although the efficacy of inhibition by ICRF-193 may be limited by its solubility in aqueous solution.

Doxorubicin Failed to Induce Detectable TOP2-B-DNA Complexes in Cardiomyocytes Derived from iPSCs but Did Suppress Etoposide-Induced Complex Formation. Although anthracyclines are widely used and effective anticancer drugs, their side effect profile includes potentially serious cardiac damage (van Dalen et al., 2005). Using iPSC-derived cardiomyocytes, we examined the expression of TOP2B and TOP2A by immunofluorescence. As anticipated for fully differentiated cells, only about 5% of the cardiomyocytes expressed significant levels of TOP2A, but all

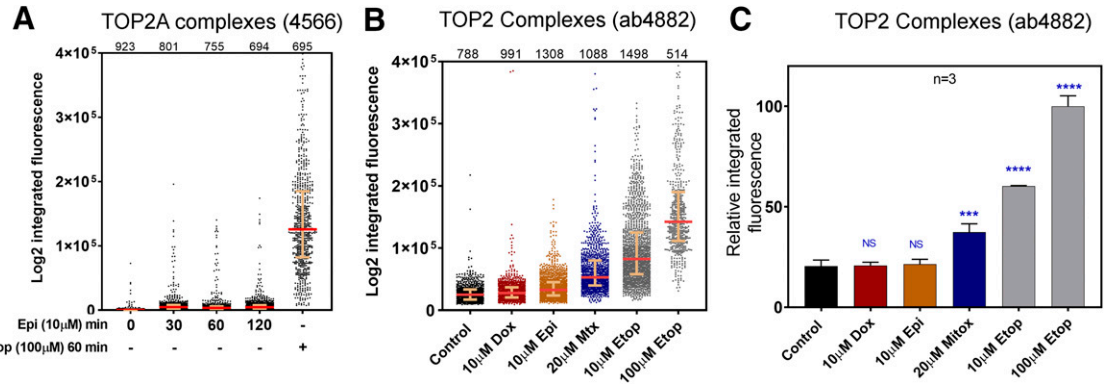

Fig. 3. Low anthracycline-induced TOP2-DNA complex TARDIS signal is not due to short drug incubation time or specific loss or masking of TOP2 C-terminal domain epitopes. (A) Cells were treated with 10 μM epi for the times indicated or with etoposide (Etop; 100 μM) for 60 minutes, and TOP2A complexes were quantified using antibody 4556 as in Fig. 1. (B and C) Cells were treated with the indicated TOP2 poisons for 60 minutes, and TOP2 complexes were analyzed using anti-TOP2 antibody 4882 (raised to N-terminal 140 kDa of calf thymus TOP2). Data are shown as scatterplots for one replica experiment (B) and as the means of the median values obtained from three replica experiments ±S.D. for (C). Significance values refer to comparison with untreated (control) cells by one-way ANOVA with Dunnett's correction for multiple comparisons. Error bars indicated S.D. values. Mtx, mitoxantrone.

cells expressed abundant TOP2B (Fig. 6A). Whereas 100 μM etoposide efficiently induced TOP2B-DNA complexes in the cardiomyocyte cells, doxorubicin did not induce TOP2B complexes significantly above background levels (Fig. 6B). Moreover, preincubation with 10 μM doxorubicin suppressed etoposide-induced TOP2B complexes in cardiomyocyte cells, confirming that doxorubicin attenuates TOP2 activity in cardiomyocytes. Thus, the inhibition observed by doxorubicin treatment is not limited to a single cell type.

In Vitro Inhibition of TOP2 Decatenation Activity by Mitoxantrone, Doxorubicin, Epirubicin, or ICRF-193. In vitro, TOP2 decatenation activity can be analyzed using highly catenated kDNA. As shown in Fig. 7, high-molecular-weight kDNA remains in the well of an agarose gel (first lane of each panel), and in the absence of drugs, TOP2A and TOP2B catalyze the decatenation of kDNA, resulting in the migration of decatenated circles into the gel (second lane of each panel). However, addition of mitoxantrone, dox, or epi resulted in a decline in the TOP2-mediated decatenation activity with increasing concentrations of drugs (Fig. 7). The effect of the catalytic inhibitor ICRF-193 is shown for comparison.

In Vitro Attenuation of Etoposide-Induced DNA Cleavage by Mitoxantrone, Doxorubicin, or Epirubicin. Data generated using two leukemia cell lines (NB4 and K562) and iPSC-derived cardiomyocytes strongly suggest that mitoxantrone, dox, and epi attenuate TOP2 activity, thereby

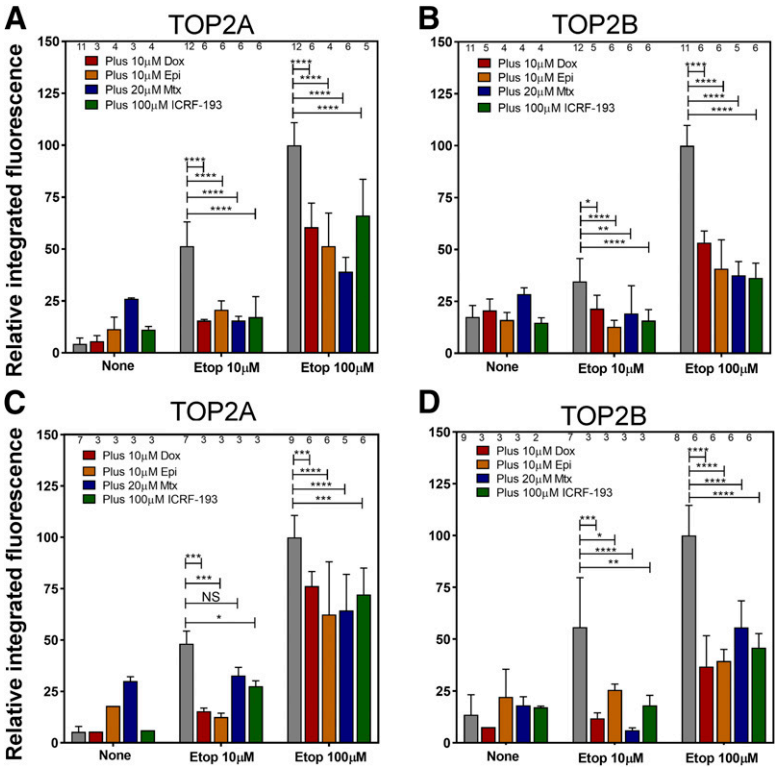

Fig. 4. Anthracyclines and mitoxantrone inhibit etoposide-induced TOP2A- and TOP2B-DNA complex stabilization. NB4 cells (A and B) or K562 cells (C and D) were preincubated for 1 hour with doxorubicin (Dox), epirubicin (Epi), mitoxantrone (Mtx), or ICRF-193 at the concentration shown in the top-left corner of each graph. Cells were then treated with 10 or 100 μM etoposide (Etop; or vehicle control) for a further hour. TOP2A (A and C) and TOP2B (B and D) complexes were quantified as in Fig. 1. The first bar in each group (gray) corresponds to treatment with etoposide alone. Data in each graph are the means of the medians from replica experiments ±S.D. The number of replicates for each condition is shown at the top of each graph. Significance tests were performed by two-way ANOVA using Dunnett's correction for multiple comparisons (comparisons were made to etoposide treatment alone).

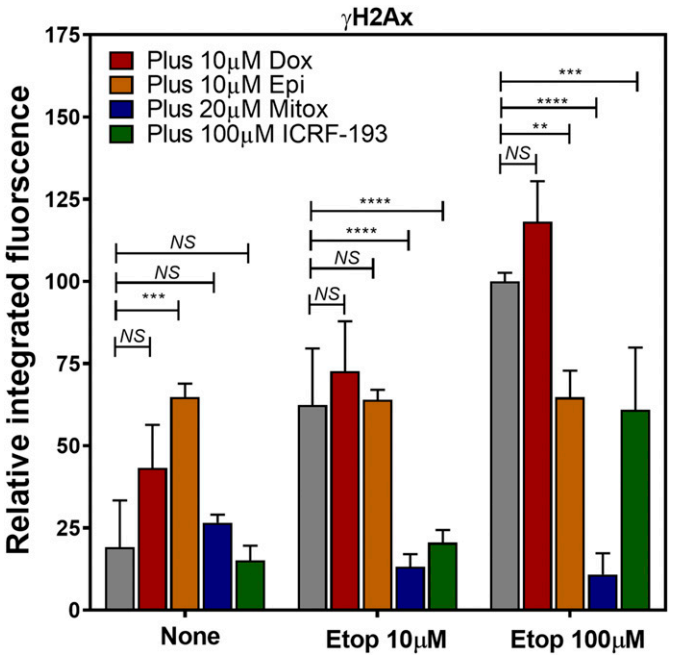

Fig. 5. Anthracyclines and mitoxantrone (Mitox) inhibit etoposide (Etop)-induced H2AX phosphorylation. NB4 cells were pretreated with anthracyclines, mitoxantrone, or ICRF-193 before treatment with etoposide, as in Fig 4. Histone H2AX phosphorylation was assessed by quantitative immunofluorescence. Data in each graph are the means of the medians from replica experiments ±S.D. Significance tests were performed as for Fig. 4.

blocking the formation of the TOP2-DNA covalent complex which prevents the action of the TOP2 poison, etoposide (Figs. 4–6). To further clarify this, we conducted in vitro DNA cleavage assays to analyze the effects of etoposide-induced TOP2-mediated DNA cleavage in the presence of mitoxantrone, dox, or epi. Cleavage experiments were performed using supercoiled plasmid DNA substrate TCS1 in the presence of etoposide and with varying concentrations of mitoxantrone, dox, or epi. Increasing concentrations of mitoxantrone, doxorubicin, or epirubicin attenuated etoposide-induced plasmid cleavage in a concentration-dependent manner (Fig. 8). Etoposide-induced DNA cleavage of both isoforms was reduced by 50% or greater at concentrations between 4 and 6 μM mitoxantrone, doxorubicin, or epirubicin.

Discussion

This study aimed to evaluate the possible consequences of combining several TOP2-targeting drugs, some of them used in combination in current treatment protocols, in cancer cells with differing characteristics and in iPSC-derived human cardiomyocytes. We used the TARDIS assay to investigate the poisoning of TOP2-DNA complexes by the clinically relevant anthracyclines, doxorubicin and epirubicin, as well as the anthracenedione mitoxantrone. Stabilized TOP2-DNA complexes were detected, albeit at low levels, following treatment of NB4 cells with doxorubicin or epirubicin, consistent with earlier studies.

Unlike etoposide, which stabilized TOP2-DNA complexes in a concentration-dependent manner in NB4 cells, mitoxantrone produced a bell-shaped curve whereby levels of TOP2A- and TOP2B-DNA complexes increase up to 10 μM but were lower at 20 μM. This suggests that mitoxantrone acts as a TOP2 poison at lower concentrations and has inhibitory activity at higher concentrations, as previously shown for idarubicin (Willmore et al., 2002). Willmore and colleagues also demonstrated inhibition by idarubicin using the TARDIS competition assay. Specifically, preincubation of cells with higher concentrations of idarubicin inhibited the etoposide-induced stabilization of TOP2-DNA complexes. In the current study, we also used the TARDIS competition assay to evaluate the activity of doxorubicin, epirubicin, and mitoxantrone as inhibitors for both isoforms of TOP2. TOP2 catalytic inhibitors reduce the level of etoposide-stabilized complexes, as they result in fewer "active" TOP2 molecules to bind and cleave DNA. Indeed, preincubation with ICRF-193, a well established catalytic inhibitor of TOP2, substantially reduced the level of etoposide-induced TOP2 poisoning. Preincubation with doxorubicin, epirubicin, or mitoxantrone also significantly reduced levels of etoposide-induced TOP2A- and TOP2B-DNA complexes (Fig. 4). This supports the notion that anthracyclines and mitoxantrone can attenuate TOP2 activity, as suggested previously by in vitro cleavage studies (Capranico et al., 1990a,b). As doxorubicin, epirubicin, and mitoxantrone are DNA intercalators, the inhibition observed at higher concentrations may be due to DNA intercalation reducing access to DNA rather than direct enzyme inhibition as observed with ICRF-193. Consistent with this, Bodley et al. (1989) demonstrated that inhibition of TOP2-mediated DNA cleavage by a series of doxorubicin and daunorubicin

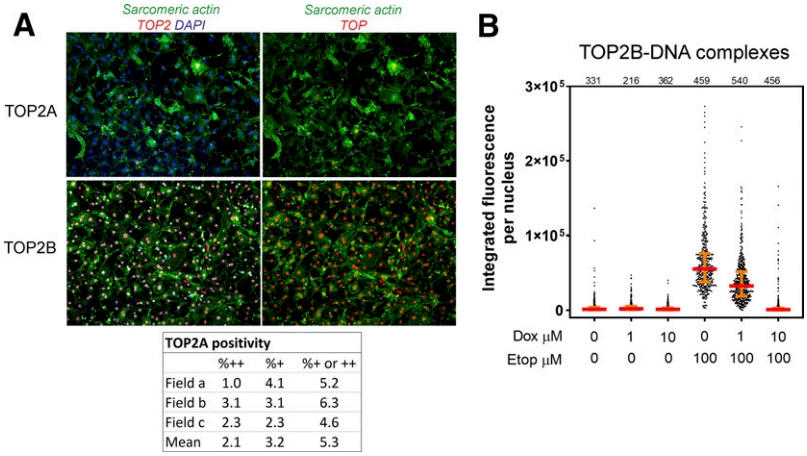

TOP2A positivity			
	%++	%+	%+ or ++
Field a	1.0	4.1	5.2
Field b	3.1	3.1	6.3
Field c	2.3	2.3	4.6
Mean	2.1	3.2	5.3

Fig. 6. TOP2 expression and induction of stable TOP2B-DNA complexes in human cardiomyocytes. (A) Induced human iPSC cardiomyocytes were stained with anti-sarcomeric actin (green) and TOP2A or TOP2B antibodies (red) and counterstained with DAPI (blue). All cells stained positive for TOP2B. Most cells were negative for TOP2A; the proportion of cells weakly (+) or strongly (++) positive for TOP2A are indicated in the table below (A). (B) Cardiomyocytes were pretreated with doxorubicin as indicated and then incubated with 100 μM etoposide (Etop). TOP2B-DNA stabilized complexes were then quantified using the TARDIS assay as in Fig. 1. Significance values refer to comparison with control (untreated) cells (Kruskal-Wallace test with Dunn's correction for multiple comparisons).

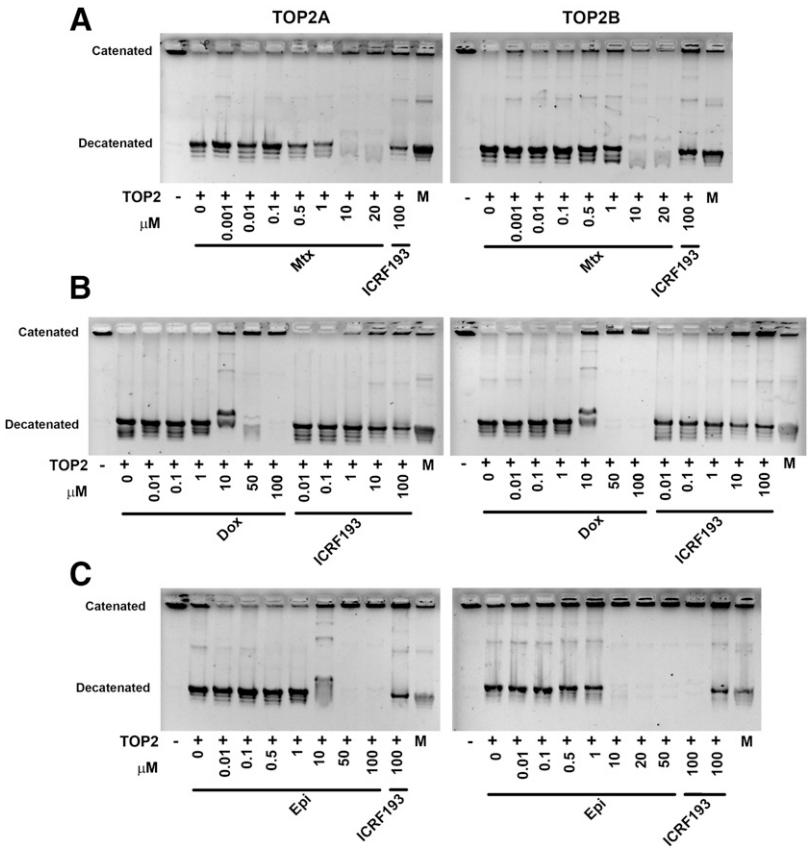

Fig. 7. Mitoxantrone, doxorubicin, and epirubicin inhibit TOP2A- and TOP2B-mediated in vitro decatenation activity. kDNA decatenation assays using recombinant TOP2A (left panels) or recombinant TOP2B (right panels) were performed in the presence of mitoxantrone (Mtx) (A), doxorubicin (B), or epirubicin (C). The gel positions of catenated and decatenated kDNA are indicated. The last lane in each gel (M) contains a marker consisting of catenated and decatenated kDNA.

congeners correlated with their intercalating capacity. In the present study (Fig. 7), we have shown that mitoxantrone, doxorubicin, and epirubicin each inhibit TOP2A- or TOP2B-mediated decatenation of kinetoplast DNA, an assay used to show inhibition of TOP2. Inhibition of TOP2B-catalyzed decatenation by doxorubicin was previously reported (Frank et al., 2016), and inhibition of TOP2A- and TOP2B-catalyzed decatenation was shown for doxorubicin, pixantrone, and etoposide by Hasinoff et al. (2016). We also show that in vitro cleavage of supercoiled plasmid DNA by etoposide is attenuated by mitoxantrone, doxorubicin, or epirubicin in a dose-dependent manner (Fig. 8); these in vitro experiments show effects at concentrations comparable to the cell-based assays and in patients. Notably, patient-derived C_{max} concentrations for mitoxantrone, doxorubicin, and epirubicin were 0.7, 7, and 17 μM, respectively(Liston and Davis, 2017) and are comparable to the concentrations that attenuate etoposide cleavage (shown in Fig. 8).

The inhibition of TOP2 by doxorubicin, epirubicin, and mitoxantrone was also investigated using the γH2AX assay to measure levels of drug-induced double-strand DNA breaks. While etoposide induced the phosphorylation of histone H2AX in a concentration-dependent manner, γH2AX levels decrease with increasing concentrations of mitoxantrone above 1 μM. This is consistent with TARDIS data showing the decrease in TOP2-DNA complex levels at higher concentrations of mitoxantrone. Consistently, levels of etoposide-induced histone H2AX phosphorylation are significantly reduced when cells are preincubated with 20 μM mitoxantrone. In contrast, levels of doxorubicin-induced DSBs increased in a concentration-dependent manner. Furthermore, preincubation with doxorubicin did not affect the levels of etoposide-induced DSBs, despite significantly reducing levels of etoposide-induced TOP2-DNA complexes as measured by TARDIS assay. This supports the idea that doxorubicin-induced DNA damage occurs via additional mechanisms beyond TOP2 poisoning,

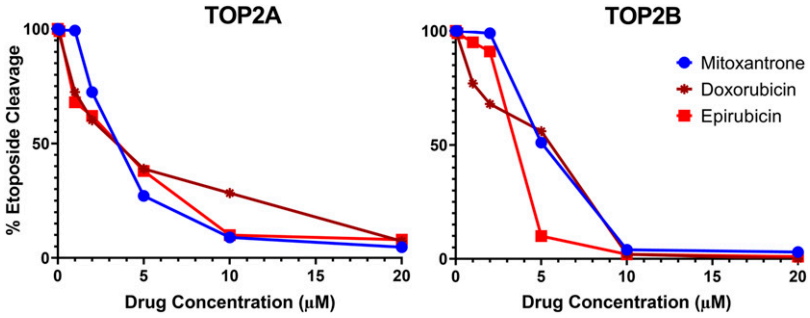

Fig. 8. Increasing doses of mitoxantrone, epirubicin, or doxorubicin attenuate etoposide-induced in vitro DNA cleavage activity. Plasmid (pTCS1) cleavage assays were performed using recombinant TOP2A or TOP2B in the presence of 1 mM etoposide combined with a range of concentrations of mitoxantrone, doxorubicin, or epirubicin. Gels were quantified, and the degree of cleavage was normalized to that obtained with etoposide alone.

which could include DNA-adduct and free-radical formation (Gewirtz, 1999; Swift et al., 2006; Coldwell et al., 2008). This contrasts with mitoxantrone and ICRF-193, which significantly reduce the etoposide-induced γH2AX signal (Fig. 5), consistent with their action predominantly through TOP2.

Anthracyclines are used in many successful treatment protocols. However, patients treated with anthracyclines such as doxorubicin and epirubicin can develop serious cardiac complications, even at doses under the maximum recommended exposure limit. The mechanisms of cardiac toxicity are elusive, and many theories have been suggested because anthracyclines appear to act on more than one target. Whereas etoposide performs its cytotoxic action by mainly targeting TOP2 (Chen et al., 1984; Minocha and Long, 1984), it is believed that the anthracyclines (doxorubicin, epirubicin) and mitoxantrone use other mechanisms in addition to TOP2 poisoning for cytotoxicity (Tuteja et al., 1997; Gewirtz, 1999; Minotti et al., 2004; Evison et al., 2016). For example, doxorubicin treatment causes marked damage to mitochondria, yet mitochondrial targeting of doxorubicin eliminated the cardiac toxicity (Jean et al., 2015). Studies in murine cardiomyocytes and human pluripotent stem cell–derived cardiomyocytes have strongly implicated TOP2B in doxorubicin-induced cardiotoxicity (Zhang et al., 2012; Maillet et al., 2016). Lyu et al. (2007) proposed a model for the role of TOP2B in cardiotoxicity, where anthracycline-induced TOP2B-DNA covalent complexes are processed via proteasomal activity to exposed DNA-DSBs in cardiomyocytes. However, this study did not directly demonstrate the presence of anthracycline-induced TOP2-DNA complexes, and as we demonstrate here in lymphoblastoid cells, TOP2B-DNA complexes are induced very inefficiently in cells by anthracyclines. This suggests that the role of TOP2B in anthracycline-induced cardiotoxicity may be less straightforward. Elucidating the mechanism by which TOP2B expression leads to doxorubicin-induced cardiotoxicity may inform cardioprotection strategies in the clinic. To further examine the possible effects of anthracyclines in light of their complicated mechanisms of TOP2 inhibition, we used iPSC-derived cardiomyocytes. Although these cells might show differences from the adult cardiomyocyte phenotype, mainly in terms of their metabolism, we show that most iPSC-derived cardiomyocytes do not express TOP2A, whereas TOP2B was expressed in all cardiomyocytes, which should also be true for adult terminally differentiated cardiomyocytes. In our experiments, doxorubicin (1 or 10 μM) did not induce TOP2B-DNA complexes above the background level in cardiomyocytes, even though complexes were efficiently induced by etoposide (Fig. 6). Furthermore, as was observed in NB4 and K562 cells, doxorubicin inhibited etoposide-induced TOP2B complex formation. This suggests that the mechanism of doxorubicin-mediated cardiotoxicity may involve inhibition of the normal cellular functions of TOP2B, such as transcriptional regulation, as opposed to TOP2B poisoning (Fig. 6). Given that TOP2A plays a major part in the cell death of cancer cells during anthracycline-containing chemotherapy while TOP2B appears less significant (Toyoda et al., 2008; Lee et al., 2016), the development of TOP2A-specific drugs may provide a means to reduce TOP2B-associated cardiotoxicity caused by anthracycline therapy (Mariani et al., 2015; Hasinoff et al., 2016) while maintaining drug efficacy.

The findings presented in this article have potential clinical implications as doxorubicin, epirubicin, and mitoxantrone are used in combination therapy with etoposide in a number of treatment regimes. In some regimes, etoposide is given concurrently with doxorubicin, epirubicin, or mitoxantrone. For example, dose-adjusted EPOCH, which is used to treat primary mediastinal lymphoma, contains rituximab, etoposide phosphate, prednisone, vincristine sulfate (Oncovin), cyclophospamide and doxorubicin hydrochloride (hydroxydaunorubicin); In dose-adjusted EPOCH doxorubicin and etoposide are actually mixed in a single bag and infused together (Wilson et al., 2002). Even when the drugs are given sequentially, they could still be present at the same time as etoposide due to their long half-lives (14.2 hours for doxorubicin, 17 hours for mitoxantrone, and 33.7 hours for epirubicin) (Liston and Davis, 2017) and, therefore, may reduce its effectiveness. The data generated herein show that use of etoposide in combination with anthracyclines or mitoxantrone reduces the activity of etoposide as a TOP2 poison and thus has the potential to reduce the efficacy of drug combinations.

Acknowledgments

We thank Anna Jirkovská, Thomas Nicholls, Roderick Skinner, Simon Bomken, and Gareth Veal for helpful discussions.

Authorship Contributions

Participated in research design: Atwal, Cowell, Austin.
Conducted experiments: Atwal, Swan, Rowe, K. Lee.
Contributed new reagents or analytic tools: D. Lee, Armstrong.
Performed data analysis: Atwal, Rowe, Cowell.
Wrote or contributed to the writing of the manuscript: Atwal, Swan, Cowell, Austin.

References

Atwal M, Lishman EL, Austin CA, and Cowell IG (2017) Myeloperoxidase enhances etoposide and mitoxantrone-mediated DNA damage: a target for myeloprotection in cancer chemotherapy. *Mol Pharmacol* **91**:49–57.
Austin CA, Barot HA, Margerrison EE, Turcatti G, Wingfield P, Hayes MV, and Fisher LM (1990) Structure and partial amino acid sequence of calf thymus DNA topoisomerase II: comparison with other type II enzymes. *Biochem Biophys Res Commun* **170**:763–768.
Binaschi M, Farinosi R, Austin CA, Fisher LM, Zunino F, and Capranico G (1998) Human DNA topoisomerase IIalpha-dependent DNA cleavage and yeast cell killing by anthracycline analogues. *Cancer Res* **58**:1886–1892.
Bodley A, Liu LF, Israel M, Seshadri R, Koseki Y, Giuliani FC, Kirschenbaum S, Silber R, and Potmesil M (1989) DNA topoisomerase II-mediated interaction of doxorubicin and daunorubicin congeners with DNA. *Cancer Res* **49**:5969–5978.
Capranico G, De Isabella P, Tinelli S, Bigioni M, and Zunino F (1993) Similar sequence specificity of mitoxantrone and VM-26 stimulation of in vitro DNA cleavage by mammalian DNA topoisomerase II. *Biochemistry* **32**:3038–3046.
Capranico G, Kohn KW, and Pommier Y (1990a) Local sequence requirements for DNA cleavage by mammalian topoisomerase II in the presence of doxorubicin. *Nucleic Acids Res* **18**:6611–6619.
Capranico G, Zunino F, Kohn KW, and Pommier Y (1990b) Sequence-selective topoisomerase II inhibition by anthracycline derivatives in SV40 DNA: relationship with DNA binding affinity and cytotoxicity. *Biochemistry* **29**:562–569.
Chen GL, Yang L, Rowe TC, Halligan BD, Tewey KM, and Liu LF (1984) Nonintercalative antitumor drugs interfere with the breakage-reunion reaction of mammalian DNA topoisomerase II. *J Biol Chem* **259**:13560–13566.
Classen S, Olland S, and Berger JM (2003) Structure of the topoisomerase II ATPase region and its mechanism of inhibition by the chemotherapeutic agent ICRF-187. *Proc Natl Acad Sci USA* **100**:10629–10634.
Coldwell KE, Cutts SM, Ognibene TJ, Henderson PT, and Phillips DR (2008) Detection of Adriamycin-DNA adducts by accelerator mass spectrometry at clinically relevant Adriamycin concentrations. *Nucleic Acids Res* **36**:e100.
Cowell IG and Austin CA (2012) Mechanism of generation of therapy related leukemia in response to anti-topoisomerase II agents. *Int J Environ Res Public Health* **9**:2075–2091.
Cowell IG, Tilby MJ, and Austin CA (2011) An overview of the visualisation and quantitation of low and high MW DNA adducts using the trapped in agarose DNA immunostaining (TARDIS) assay. *Mutagenesis* **26**:253–260.
De Angelis A, Urbanek K, Cappetta D, Piegari E, Ciuffreda LP, Rivellino A, Russo R, Esposito G, Rossi F, and Berrino L (2016) Doxorubicin cardiotoxicity and target cells: a broader perspective. *Cardiooncology* **2**:2.
Dubois NC, Craft AM, Sharma P, Elliott DA, Stanley EG, Elefanty AG, Gramolini A, and Keller G (2011) SIRPA is a specific cell-surface marker for isolating cardiomyocytes derived from human pluripotent stem cells. *Nat Biotechnol* **29**: 1011–1018.

Errington F, Willmore E, Leontiou C, Tilby MJ, and Austin CA (2004) Differences in the longevity of topo IIalpha and topo IIbeta drug-stabilized cleavable complexes and the relationship to drug sensitivity. *Cancer Chemother Pharmacol* **53**:155–162.
Errington F, Willmore E, Tilby MJ, Li L, Li G, Li W, Baguley BC, and Austin CA (1999) Murine transgenic cells lacking DNA topoisomerase IIbeta are resistant to acridines and mitoxantrone: analysis of cytotoxicity and cleavable complex formation. *Mol Pharmacol* **56**:1309–1316.
Evison BJ, Sleebs BE, Watson KG, Phillips DR, and Cutts SM (2016) Mitoxantrone, more than just another topoisomerase II poison. *Med Res Rev* **36**:248–299.
Ferrazzi E, Woynarowski JM, Arakali A, Brenner DE, and Beerman TA (1991) DNA damage and cytotoxicity induced by metabolites of anthracycline antibiotics, doxorubicin and idarubicin. *Cancer Commun* **3**:173–180.
Frank NE, Cusack BJ, Talley TT, Walsh GM, and Olson RD (2016) Comparative effects of doxorubicin and a doxorubicin analog, 13-deoxy, 5-iminodoxorubicin (GPX-150), on human topoisomerase IIβ activity and cardiac function in a chronic rabbit model. *Invest New Drugs* **34**:693–700.
Gewirtz DA (1999) A critical evaluation of the mechanisms of action proposed for the antitumor effects of the anthracycline antibiotics adriamycin and daunorubicin. *Biochem Pharmacol* **57**:727–741.
Hasinoff BB, Wu X, Patel D, Kanagasabai R, Karmahapatra S, and Yalowich JC (2016) Mechanisms of action and reduced cardiotoxicity of pixantrone; a topoisomerase II targeting agent with cellular selectivity for the topoisomerase IIα Isoform. *J Pharmacol Exp Ther* **356**:397–409.
Huelsenbeck SC, Schorr A, Roos WP, Huelsenbeck J, Henninger C, Kaina B, and Fritz G (2012) Rac1 protein signaling is required for DNA damage response stimulated by topoisomerase II poisons. *J Biol Chem* **287**:38590–38599.
Jean SR, Tulumello DV, Riganti C, Liyanage SU, Schimmer AD, and Kelley SO (2015) Mitochondrial targeting of doxorubicin eliminates nuclear effects associated with cardiotoxicity. *ACS Chem Biol* **10**:2007–2015.
Lanotte M, Martin-Thouvenin V, Najman S, Balerini P, Valensi F, and Berger R (1991) NB4, a maturation inducible cell line with t(15;17) marker isolated from a human acute promyelocytic leukemia (M3). *Blood* **77**:1080–1086.
Lee KC, Bramley RL, Cowell IG, Jackson GH, and Austin CA (2016) Proteasomal inhibition potentiates drugs targeting DNA topoisomerase II. *Biochem Pharmacol* **103**:29–39.
Lee MP, Sander M, and Hsieh TS (1989) Single strand DNA cleavage reaction of duplex DNA by Drosophila topoisomerase II. *J Biol Chem* **264**:13510–13518.
Lian X, Zhang J, Azarin SM, Zhu K, Hazeltine LB, Bao X, Hsiao C, Kamp TJ, and Palecek SP (2013) Directed cardiomyocyte differentiation from human pluripotent stem cells by modulating Wnt/β-catenin signaling under fully defined conditions. *Nat Protoc* **8**:162–175.
Liston DR and Davis M (2017) Clinically relevant concentrations of anticancer drugs: a guide for nonclinical studies. *Clin Cancer Res* **23**:3489–3498.
Long BH, Musial ST, and Brattain MG (1984) Comparison of cytotoxicity and DNA breakage activity of congeners of podophyllotoxin including VP16-213 and VM26: a quantitative structure-activity relationship. *Biochemistry* **23**:1183–1188.
Lown JW, Hanstock CC, Bradley RD, and Scraba DG (1984) Interactions of the antitumor agents mitoxantrone and bisantrene with deoxyribonucleic acids studied by electron microscopy. *Mol Pharmacol* **25**:178–184.
Lozzio CB and Lozzio BB (1975) Human chronic myelogenous leukemia cell-line with positive Philadelphia chromosome. *Blood* **45**:321–334.
Lyu YL, Kerrigan JE, Lin C-P, Azarova AM, Tsai Y-C, Ban Y, and Liu LF (2007) Topoisomerase IIbeta mediated DNA double-strand breaks: implications in doxorubicin cardiotoxicity and prevention by dexrazoxane. *Cancer Res* **67**:8839–8846.
Maillet A, Tan K, Chai X, Sadananda SN, Mehta A, Ooi J, Hayden MR, Pouladi MA, Ghosh S, Shim W, et al. (2016) Modeling doxorubicin-induced cardiotoxicity in human pluripotent stem cell derived-cardiomyocytes. *Sci Rep* **6**:25333.
Mariani A, Bartoli A, Atwal M, Lee KC, Austin CA, and Rodriguez R (2015) Differential targeting of human topoisomerase II isoforms with small molecules. *J Med Chem* **58**:4851–4856.
Minocha A and Long BH (1984) Inhibition of the DNA catenation activity of type II topoisomerase by VP16-213 and VM26. *Biochem Biophys Res Commun* **122**: 165–170.
Minotti G, Menna P, Salvatorelli E, Cairo G, and Gianni L (2004) Anthracyclines: molecular advances and pharmacologic developments in antitumor activity and cardiotoxicity. *Pharmacol Rev* **56**:185–229.
Montaudon D, Pourquier P, Denois F, de Tinguy-Moreaud E, Lagarde P, and Robert J (1997) Differential stabilization of topoisomerase-II-DNA cleavable complexes by doxorubicin and etoposide in doxorubicin-resistant rat glioblastoma cells. *Eur J Biochem* **245**:307–315.
Nitiss JL, Soans E, Rogojina A, Seth A, and Mishina M (2012) Topoisomerase assays. *Curr Protoc Pharmacol* **57**:Unit3.31-3.3.27.
Patel S, Jazrawi E, Creighton AM, Austin CA, and Fisher LM (2000) Probing the interaction of the cytotoxic bisdioxopiperazine ICRF-193 with the closed enzyme clamp of human topoisomerase IIalpha. *Mol Pharmacol* **58**:560–568.
Pommier Y, Leo E, Zhang H, and Marchand C (2010) DNA topoisomerases and their poisoning by anticancer and antibacterial drugs. *Chem Biol* **17**:421–433.
Reichardt P, Tabone M-D, Mora J, Morland B, and Jones RL (2018) Risk-benefit of dexrazoxane for preventing anthracycline-related cardiotoxicity: re-evaluating the European labeling. *Future Oncol* **14**:2663–2676.
Roca J, Ishida R, Berger JM, Andoh T, and Wang JC (1994) Antitumor bisdioxopiperazines inhibit yeast DNA topoisomerase II by trapping the enzyme in the form of a closed protein clamp. *Proc Natl Acad Sci USA* **91**:1781–1785.
Sinha BK, Mimnaugh EG, Rajagopalan S, and Myers CE (1989) Adriamycin activation and oxygen free radical formation in human breast tumor cells: protective role of glutathione peroxidase in adriamycin resistance. *Cancer Res* **49**:3844–3848.
Smart DJ, Halicka HD, Schmuck G, Traganos F, Darzynkiewicz Z, and Williams GM (2008) Assessment of DNA double-strand breaks and gammaH2AX induced by the topoisomerase II poisons etoposide and mitoxantrone. *Mutat Res* **641**:43–47.
Sparano JA, Gray RJ, Makower DF, Pritchard KI, Albain KS, Hayes DF, Geyer CE Jr, Dees EC, Goetz MP, Olson JA Jr, et al. (2018) Adjuvant chemotherapy guided by a 21-gene expression assay in breast cancer. *N Engl J Med* **379**:111–121.
Suzuki H, Tarumoto Y, and Ohsawa M (1997) Topoisomerase II inhibitors fail to induce chromosome-type aberrations in etoposide-resistant cells: evidence for essential contribution of the cleavable complex formation to the induction of chromosome-type aberrations. *Mutagenesis* **12**:29–33.
Swift LP, Rephaeli A, Nudelman A, Phillips DR, and Cutts SM (2006) Doxorubicin-DNA adducts induce a non-topoisomerase II-mediated form of cell death. *Cancer Res* **66**:4863–4871.
Tewey KM, Rowe TC, Yang L, Halligan BD, and Liu LF (1984) Adriamycin-induced DNA damage mediated by mammalian DNA topoisomerase II. *Science* **226**: 466–468.
Tohyama S, Hattori F, Sano M, Hishiki T, Nagahata Y, Matsuura T, Hashimoto H, Suzuki T, Yamashita H, Satoh Y, et al. (2013) Distinct metabolic flow enables large-scale purification of mouse and human pluripotent stem cell-derived cardiomyocytes. *Cell Stem Cell* **12**:127–137.
Toyoda E, Kagaya S, Cowell IG, Kurosawa A, Kamoshita K, Nishikawa K, Iiizumi S, Koyama H, Austin CA, and Adachi N (2008) NK314, a topoisomerase II inhibitor that specifically targets the alpha isoform. *J Biol Chem* **283**:23711–23720.
Tuteja N, Phan TN, Tuteja R, Ochem A, and Falaschi A (1997) Inhibition of DNA unwinding and ATPase activities of human DNA helicase II by chemotherapeutic agents. *Biochem Biophys Res Commun* **236**:636–640.
van Dalen EC, Caron HN, Dickinson HO, and Kremer LCM (2005) Cardioprotective interventions for cancer patients receiving anthracyclines. *Cochrane Database Syst Rev* (1):CD003917.
Vos SM, Tretter EM, Schmidt BH, and Berger JM (2011) All tangled up: how cells direct, manage and exploit topoisomerase function. *Nat Rev Mol Cell Biol* **12**: 827–841.
Wasserman RA, Austin CA, Fisher LM, and Wang JC (1993) Use of yeast in the study of anticancer drugs targeting DNA topoisomerases: expression of a functional recombinant human DNA topoisomerase II alpha in yeast. *Cancer Res* **53**: 3591–3596.
West KL, Meczes EL, Thorn R, Turnbull RM, Marshall R, and Austin CA (2000) Mutagenesis of E477 or K505 in the B′ domain of human topoisomerase II beta increases the requirement for magnesium ions during strand passage. *Biochemistry* **39**:1223–1233.
Willmore E, Errington F, Tilby MJ, and Austin CA (2002) Formation and longevity of idarubicin-induced DNA topoisomerase II cleavable complexes in K562 human leukaemia cells. *Biochem Pharmacol* **63**:1807–1815.
Willmore E, Frank AJ, Padget K, Tilby MJ, and Austin CA (1998) Etoposide targets topoisomerase IIalpha and IIbeta in leukemic cells: isoform-specific cleavable complexes visualized and quantified in situ by a novel immunofluorescence technique. *Mol Pharmacol* **54**:78–85.
Wilson WH, Grossbard ML, Pittaluga S, Cole D, Pearson D, Drbohlav N, Steinberg SM, Little RF, Janik J, Gutierrez M, et al. (2002) Dose-adjusted EPOCH chemotherapy for untreated large B-cell lymphomas: a pharmacodynamic approach with high efficacy. *Blood* **99**:2685–2693.
Winterbourn CC, Gutteridge JM, and Halliwell B (1985) Doxorubicin-dependent lipid peroxidation at low partial pressures of O2. *J Free Radic Biol Med* **1**:43–49.
Zhang S, Liu X, Bawa-Khalfe T, Lu L-S, Lyu YL, Liu LF, and Yeh ETH (2012) Identification of the molecular basis of doxorubicin-induced cardiotoxicity. *Nat Med* **18**:1639–1642.

Address correspondence to: Ian G. Cowell, Institute for Cell and Molecular Biosciences, Newcastle University, Newcastle upon Tyne NE2 4HH, UK. E-mail: ian.cowell@ncl.ac.uk; or Caroline A. Austin, Institute for Cell and Molecular Biosciences, Newcastle University, Newcastle upon Tyne NE2 4HH, UK. E-mail: caroline.austin@ncl.ac.uk

Atwal et al Molecular Pharmacology

Supplemental Data

Intercalating TOP2 poisons attenuate topoisomerase action at higher concentrations

Mandeep Atwal, Rebecca L. Swan, Chloe Rowe, Ka C. Lee, David C Lee, Lyle Armstrong, Ian G Cowell*, Caroline A Austin*

Table of Contents

Supplemental Figure Legends

Supplemental Figure 1. Characteristics of inhouse antibodies used in this study. (A) TOP2 domain structure and location of immunogen polypeptide regions. The divergent C-terminal domains of TOP2A and TOP2B are coloured. Polyclonal antibodies 4566 & 4555 were raised in rabbits immunized with GST-fusion proteins containing amino acids 1244-1531 of TOP2A or 1263-1621 of TOP2B respectively. Polyclonal 4882 was produced in a rabbit immunized with a calf thymus TOP2 prep containing predominantly C-terminally truncated TOP2. **(B)** Western blot validation of antisera 4566 and 4555. rTOP2A & rTOP2B, recombinant TOP2A and B respectively, expressed in and purified from yeast; K562 WCE, whole cell extract derived from K562 cells; Nalm$^{TOP2B-/-}$, whole cell extract derived from TOP2B null Nalm6 cells (human pre-B leukemia cell line). **(C)** TARDIS analysis in K562 and Nalm$^{TOP2B-/-}$ cells, confirming lack of etoposide induced signal in TOP2B null Nalm$^{TOP2B-/-}$ cells (but efficient induction of signal in K562 cells) with antibody 4555, but efficient induction of signal in these cells with antibody 4566. **(D-F)** Western blot validation of antibody 4882 (note TOP2A and TOP2B frequently fail to resolve from each other in WCEs run on mini-gels). **(G)** Nuclear immunofluorescent staining pattern with antibody 4882 in WT and TOP2B null Nalm6 cells.

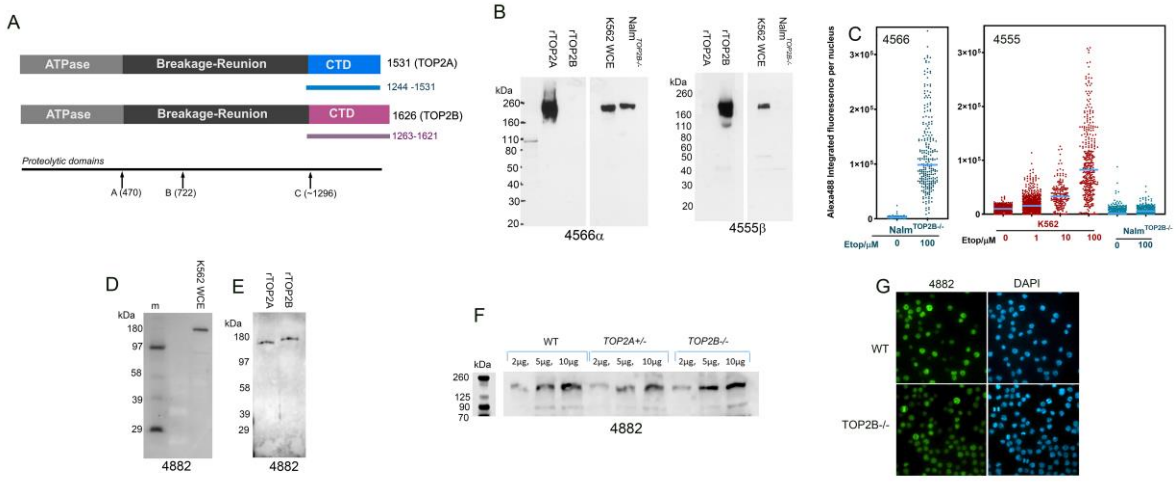

Supplemental Figure 1